RSC Advances

PAPER

View Article Online
View Journal | View Issue

Cite this: *RSC Adv.*, 2022, **12**, 16835

Template assisted preparation of silicone (polydimethylsiloxane) elastomers and their self-cleaning application

Xiaohong Ding,[a] Biya Chen,[a] Muchang Li,[a] Ruilai Liu,[a] Jinyun Zhao,[a] Jiapeng Hu,[a] Xingping Fu,[a] Yuejin Tong,*[b] Hanqing Lu[c] and Jing Lin *[c]

Received 28th April 2022
Accepted 1st June 2022

DOI: 10.1039/d2ra02583c

rsc.li/rsc-advances

The formation of self-cleaning functions on silicone elastomers is crucial for practical applications but still challenging. In this study, superhydrophobic silicone elastomers (SHSEs) with a 3D-hierarchical microstructure were achieved during the curing process with the assistance of a homemade template. The micro–nano structure formed by the assistance of the template makes the silicone elastomer surface achieve robust superhydrophobicity with a WCA at ~163°, which can easily self-clean, removing surface contamination. Also, TiO_2 particles transferred from the template endow the surface with photocatalytic functions, which can degrade organic pollutants under UV irradiation. After sandpaper abrasion, the formed SHSE can maintain its excellent hydrophobicity and show liquid repellency to wine and coffee droplets. The SHSEs with self-cleaning functions have promising applications in water treatment, medical facilities, and wearable devices.

1. Introduction

Silicone elastomers have gained considerable attention due to their broad research scope and applications in micro-fluidic reactors, soft robots, medical facilities, and wearable devices due to their excellent flexibility, hydrophobicity, visibility, and air permeability.[1–3] A self-cleaning ability is desirable since once the surfaces are contaminated with stains, extra energy or cleaning agents will be required to clean them. Typically, the self-cleaning function can be realized in two ways. One is *via* a physical process, which is to construct super-wettability surfaces to get rid of dust during water rolling or sheeting.[4,5] The other is a chemical photocatalytic process, by which photocatalysis would finally degrade organic pollutants into carbon dioxide and water under light or UV irradiation, and then the contaminants would be eventually removed.[6–10] Multifunctional surfaces are attractive since a surface with superhydrophobicity has a high water contact angle (WCA $\geq 150°$) and low sliding angle ($<10°$) and could easily remove dirt by a rolling process; meanwhile, the photocatalytic function could degrade the organic pollutants in air or water.[6,11,12]

Two essentials should be considered about realizing superhydrophobicity. One is low surface energy materials, and the other is a macro/nano-structural roughness.[13–15] Compared to multiple processes, a one-step process is more desirable for obtaining robust SHSEs as any preceding or subsequent process (such as coating) could destroy the surface micro/nano-structures, which would lead to the loss of superhydrophobicity. Several methods have been applied to achieve surface superhydrophobicity, including sol–gel methods,[16,17] laser-induced methods,[18] electrochemical methods,[19] plasma treatment,[20,21] phase separation methods,[22] spin-coating,[23] template methods.[24,25] However, robust superhydrophobicity is even more challenging since surface superhydrophobicity is slowly decreased by adhesion of oily contamination in practical uses. Once the surface was polluted, the superhydrophobicity hardly recovered without washing by organic solvent. Introducing semiconductor photocatalysis titanium (TiO_2) is probably a promising path to take off stained organics, which can be easily removed by the photocatalytic effect of TiO_2.[6–9,26] In addition, most superhydrophobic products are fragile or unable to withstand abrasion. Abrasion accelerates friction loss of underlying materials and may change the surface from superhydrophobic to hydrophobic, resulting in the pinning of the droplets to the surfaces.[27,28] Designing a surface with a micro/nanostructure to provide water repellency and durability could improve the mechanical robustness.[29]

We proposed a facile route to get SHSEs with 3D-hierarchical microstructure and photocatalysis in the present work. As shown in Fig. 1(a), the homemade template was prepared by combining an electro-etching process and a dip-coating method. During the electro-etching process, aluminum plates were immersed in HCl solution to obtain porous aluminum. The porous aluminum was then coated by TiO_2/PDMS suspension to form the homemade

[a]*Fujian Provincial Key Laboratory of Eco-Industrial Green Technology, College of Ecological and Resources Engineering, Wuyi University, 354300, Wuyishan, China*
[b]*College of Chemistry and Materials Science, Fujian Normal University, 350007, Fuzhou, China. E-mail: tongyuejinfjnu@163.com*
[c]*School of Chemistry and Chemical Engineering, Guangzhou University, Guangzhou, 510006, P. R. China. E-mail: linjin00112043@126.com; linjing@gzhu.edu.cn*

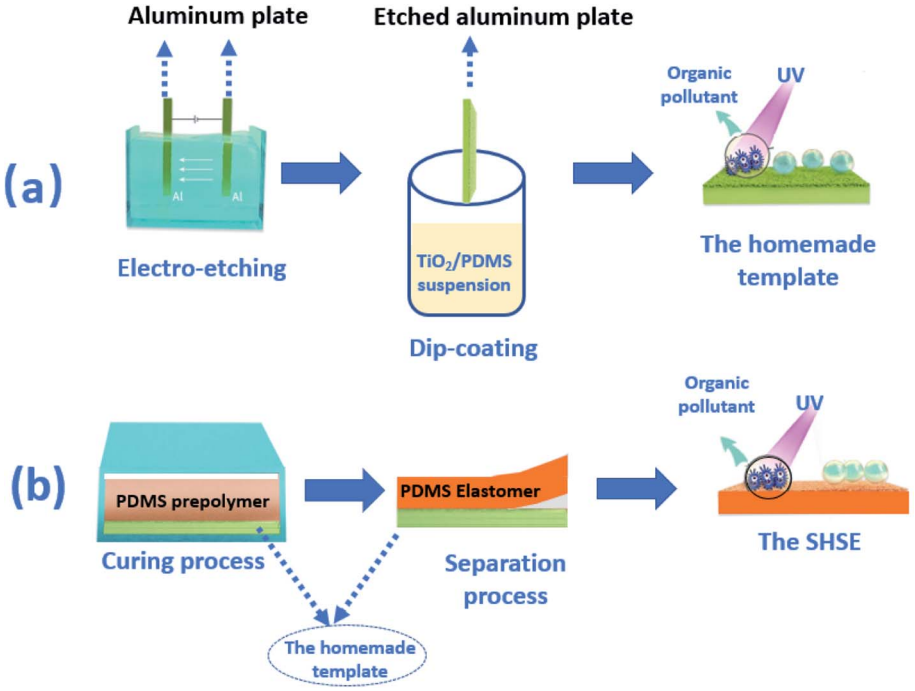

Fig. 1 Schematic of the preparation of (a) the homemade template (b) the SHSE.

template. In Fig. 1(b), commercially available PDMS prepolymer was added in a stainless-steel mold with the homemade template sticked to the mold. After curing process, PDMS became a solid rubber and then the homemade template was separated from the cured PDMS elastomer (rubber), and then the SHSE was obtained. Due to the rough surface with micro/nano-structure copied from the porous template and the low surface energy from PDMS molecules, the silicone elastomer has superhydrophobic self-cleaning properties. On the other hand, the TiO_2 particles transferred from templates make the surface possess a photocatalytic self-cleaning function. Thus, SHSEs with photocatalysis were prepared during a solidification process in stainless steel mold assisted by porous aluminum templates. This novel method will endow multi-functions on the surface of elastomers during one molding process. Furthermore, it has promising applications for extending other target functions during polymer molding processes.

2. Experimental

2.1 Preparation of the TiO_2/PDMS suspension

1 g tri-methoxy terminated polydimethylsiloxane (PDMS) was dissolved in 99 g ethyl alcohol under magnetic stirring. 6 g TiO_2 mixture of three different sizes mixed with the weight ratio of 20 nm : 100 nm : 200 nm = 1 : 1 : 1 was added into the PDMS solution under vigorous stirring, and then a TiO_2/PDMS suspension was formed.

2.2 Preparation of the homemade template

Porous aluminum plates (1.0 × 2.5 cm^2) were obtained by the electrolytic etching (in 3.6–3.7 wt% HCl solution) method at the anode under 7–8 V for 8–9 minutes. After cleaning with deionized water, the template was dipped into TiO_2/PDMS suspension for 30 seconds before it was pulled up at a speed of 1 mm s^{-1}. The as-prepared template was kept in the oven at 50 °C to form a TiO_2/PDMS coating on the porous aluminum, and then the homemade template was obtained.

2.3 Preparation of the SHSEs

The template was put on the bottom of a stainless-steel mold. Then, silicone elastomers were formed during the solidification process (100 °C, 2 hours) in an oven using Sylgard 184 Silicone elastomer base and its cross-linker (Dow Corning) in a 10 : 1 ratio. When keeping the mold in the oven and cooling it to 25 °C for 6 h to ensure sufficient curing, SHSEs with photocatalysis were achieved after separating the silicone elastomer from templates.

2.4 Characterization

X-ray photoelectron spectroscopy (XPS) was performed to determine the chemical compositions of the hybrids using a VG ESCALAB 250Xi model spectrometer (Thermo Electron, The UK). High-resolution transmission electron microscopy (HRTEM) was carried out using a Talos F2100X (Thermo Scientific, The US) to investigate the interaction between PDMS and TiO_2. X-ray diffraction spectroscopy (XRD, Rinku-Miniflex 600 Instrument, Japan) was performed to investigate the crystal form of TiO_2 in samples. Surface morphology is investigated by scanning electron microscopy (SEM, ZEISS EVO 18) and Atomic Force Microscope (AFM, JPK Instrument). The water-repellency properties of the surface of silicone elastomers were investigated by testing water contact angles (WCAs) and

water slide angles (WSAs) using a DSA25 model contact angle goniometer (KRUSS, German) with a 2.0 μL water droplet and 50.0 μL, respectively.

2.5 Sandpaper abrasion test

The superhydrophobic surface of a silicone elastomer is put bottom down and slides with a weight of 50.0 g on the sandpaper (grit no. 320) at a fixed distance. WCAs and WSAs are recorded at every 0.5 m.

2.6 Degradation of resazurin dye

During the preconditioning step, 10 mL Rz methanol solution (0.02 mmol L^{-1}) was added to the disk with samples and covered with a UV-A transparent glass plate for 12 h in the dark to ensure the surface absorbed the dye. This process was followed by monitoring the UV-vis spectra with occasional agitation of the solution (changed to 10.0 mL 0.01 mmol L^{-1} Rz) over a certain period under irradiation with UV light ($\lambda = 365$ nm).

3. Result and discuss

3.1 Composition of the TiO_2/PDMS coating on the porous aluminum

TEM images in Fig. 2(a) show that the coating is composed of micro/nano-structure particles from mixed TiO_2. We can also see PDMS laid outside the inorganic particles, which make a contribution as a low surface energy component. X-ray photoelectron spectroscopy was conducted to examine the elemental composition and the interaction between two components. From Fig. 2(b), we can see clear peaks of Si 2s and Si 2p showing up after incorporating PDMS. Furthermore, Fig. 2(c) shows that the O 1s peaks centered at 529.44 eV for oxygen atoms from Ti–O and 531.53 eV for oxygen atoms from –O–H, which is from the absorbed water molecules. The peak for oxygen atoms from Ti–O shifted to the lower binding energy of 529.1 eV. Meanwhile, the strength of the oxygen atoms from –OH in TiO_2/PDMS becomes more robust than the ones from Ti–O compared to TiO_2, which indicates that a covalent reaction happened between metal-oxide and organic PDMS.[12] Three methoxy groups from PDMS would become –OH after hydrolysis. Furthermore, –OH groups will either interact with –OH from the surface of TiO_2 or –OH from PDMS (after hydrolysis). The XRD spectra in Fig. 2(d) show that the mixed TiO_2 particles are crystallized anatase, which shows typical peaks for crystal facets of (101), (004), (112), (200), (105), (211), (204), and (200). These peaks are kept in TiO_2/PDMS, which indicates that the composite could be assumed to possess the effective photocatalytic function as TiO_2. In particular, the –OH generated from the hydrolysis of trimethoxy-terminated PDMS favors the interaction with TiO_2.

3.2 Superhydrophobicity of the homemade template

TiO_2/PDMS coatings were applied on porous substrates by directly dipping method. Although some precipitation occurred, we can shake the container by hand to disperse the precipitated particles before the practice. We can see the

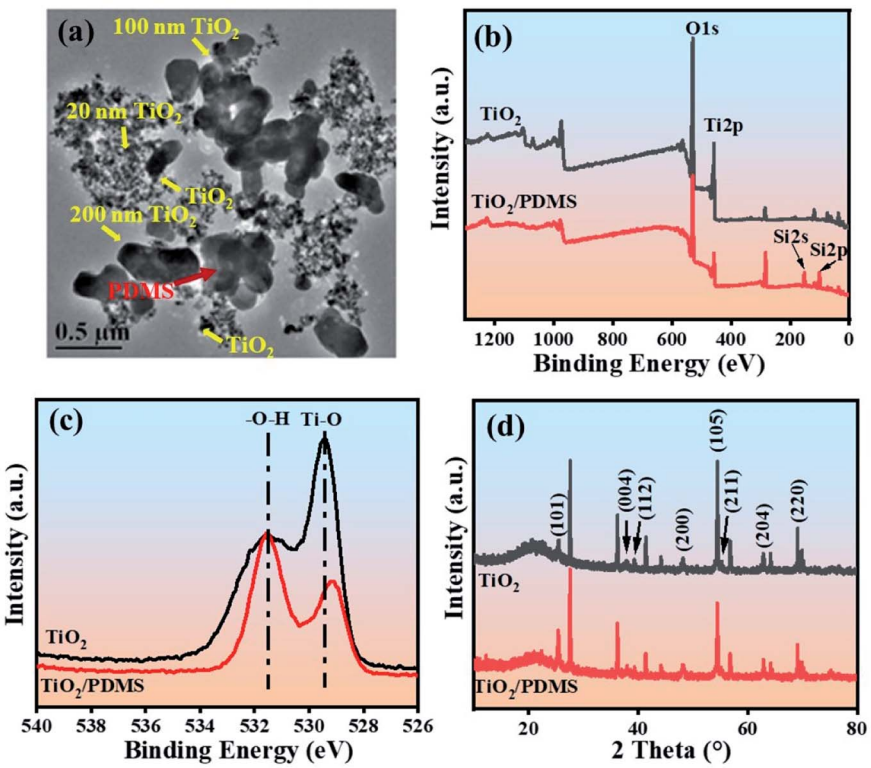

Fig. 2 (a) TEM images of as-prepared TiO_2/PDMS, (b) XPS wide-scan survey spectrum of TiO_2 and TiO_2/PDMS, (c) high-resolution scan of the O 1s peak (d) XRD spectra of TiO_2 and TiO_2/PDMS.

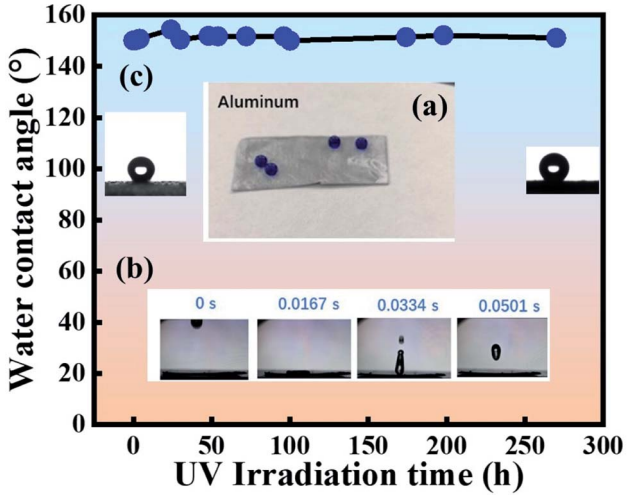

Fig. 3 (a) Water droplets sitting on TiO_2/PDMS coating treated substrates, (b) time-lapse photographs of water droplets bouncing on TiO_2/PDMS treated substrates, (c) water contact angle on TiO_2/PDMS treated glass as a function of UV irradiation time.

droplets sitting well on TiO_2/PDMS treated surface in Fig. 3(a). Thus, TiO_2/PDMS coated surface shows a highly water-repellency property. The water bouncing test (Fig. 3(b)) demonstrates that the water droplets can quickly bounce on the surface, indicating that the surface is superhydrophobic other than uncoated porous substrates. The UV irradiation test [Fig. 3(c)] show that the WCAs can last unchanged (above 150°) over 270 hours under UV irradiation. All the above results indicate that the as-prepared TiO_2/PDMS coating is superhydrophobic and has self-cleaning potential.[30,31]

3.3 Morphology characterization of the homemade template and the SHSE

PDMS is hydrophobic with low surface energy at 21–22 mN m^{-1}, and its intrinsic water contact angle is ~110°. Roughness makes it possible for a droplet to have more than one metastable equilibrium position. The droplet can transfer from one metastable equilibrium to another if the energy barrier can be overcome.[13] As shown in Fig. 4(a), after the etching of the aluminum plate, a 3D-hierarchical porous structure is presented in the etched aluminum plate. After the dipping process, we can see the coating accumulating on the porous aluminum plate while the hierarchical structures remain [Fig. 4(b)], and the initial WCA is 160°. We can see from Fig. 4(c) that the silicone elastomer has a 3D-hierarchical structure with an initial WCA of 163°, which was copied from the template. However, the

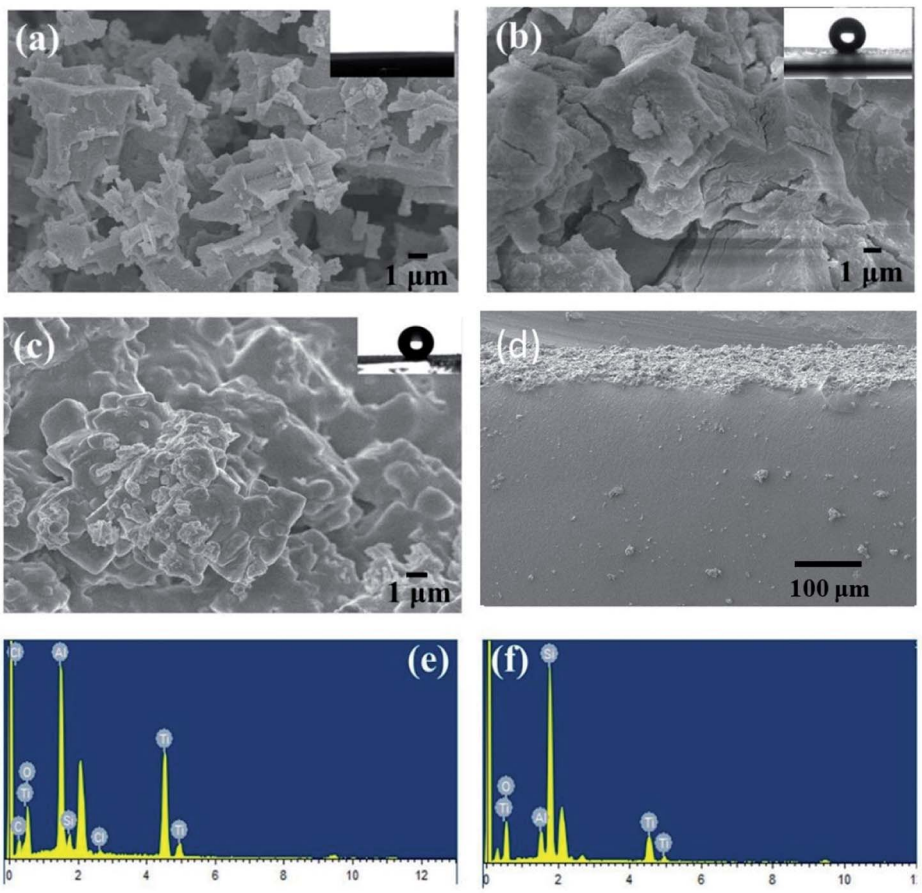

Fig. 4 SEM images of (a) etched porous aluminum plate, (b) the coated porous aluminum template, (c) silicone elastomer surface after separating from templates; insets are WCA images after dropping a 2 μL water droplet on the surfaces; (d) side-on silicone elastomer image, (e and f) EDS elemental analysis of the coated porous aluminum template and silicone elastomer after separating from templates.

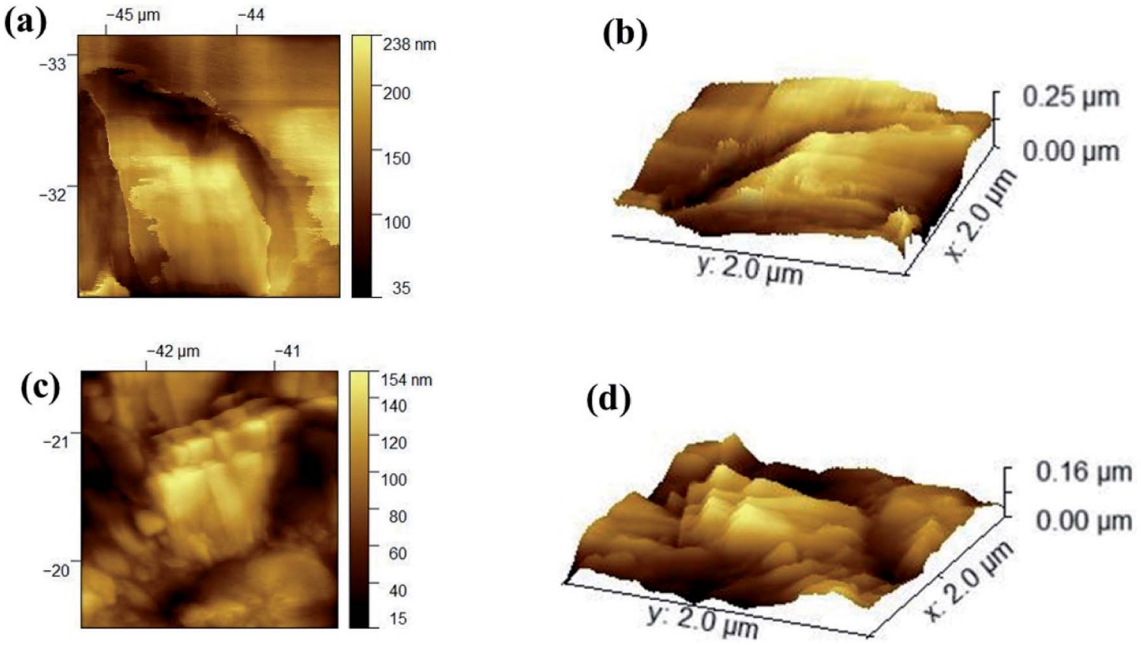

Fig. 5 The AFM images of silicone elastomers formed with (a and b) plane aluminum, (c and d) the homemade template.

porous structure was lost due to the cross-linking reaction during the curing process. Compared to the inner part of the silicone elastomer, we can see a clear roughness structure from the side-on image in Fig. 4(d). We can also see that the inner part of the silicone elastomer has an intact structure, so the template had only worked on the surface of the silicone elastomer. From Fig. 4(e and f), we can see from the EDS elemental analysis that Ti element exists on both template and the

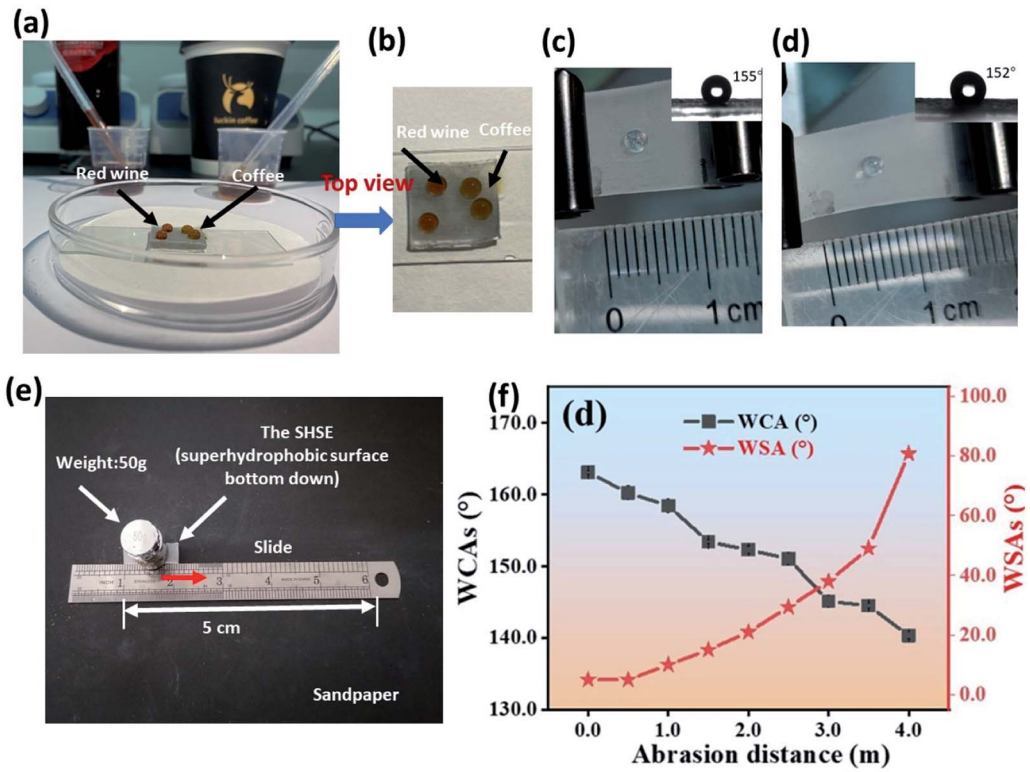

Fig. 6 (a) Side view and (b) top view images of the superhydrophobic effect proved by red wine and coffee; superhydrophobicity test (c) before and (d) after stretching to 130%; (e) schematic diagram of sandpaper abrasion test. (f) WCAs and WSAs after each abrasion test.

template-assisted silicone elastomer, which comes from the nano-TiO_2. AFM results presented in Fig. 5(c and d) proved that the roughness of template-assisted preparation silicone increased compared to the silicone formed without the template in Fig. 5(a and b), which was consistent with the SEM results. The result indicated that both the hierarchical structure and the component (TiO_2 particles) could be successfully transferred from the template.

3.4 Liquid repellency and wear resistance of the SHSE

Other than water droplets, the as-prepared silicone elastomers showed liquid repellency. As presented in Fig. 6(a and b), we can see both wine and coffee droplets can sit by a round shape on the surface of the SHSE. As it is shown in Fig. 6(c and d), before stretching, the water droplet is round and the WCA is 155° for the SHSE. After stretching the SHSE to 130%, the water droplet is also round with a WCA at 152°. This result indicated that the superhydrophobicity of the bulk elastomer is kept during stretching, which shows potential self-cleaning application when deformation occurred. In addition, we carried out the sandpaper abrasion test to explore the robustness and anti-abrasive feature of superhydrophobic elastomers (Fig. 6(c)). It presents in Fig. 6(d) that the initial WCA and WSA of SHSE are 163° and 5° separately. Both have no obvious change, with the abrasion distance increasing from 0 to 1.0 m (Fig. 6(b)). After moving 1.0 m, the WCAs gradually decrease while WSAs increase. After 3.5 m, the WCA decreases to 140.3° with a WSA at 80.7°. Thus, the superhydrophobic elastomer can maintain its excellent liquid repellency after sandpaper abrasion.

3.5 Self-cleaning performance of the homemade template and the SHSE

WCAs test against UV irradiation time was recorded to evaluate the UV duration. The initial water contact angle for the untreated silicone elastomer, the template and the SHSE were 114°, 160° and 163°, respectively, as shown in Fig. 7(a1, a3 and a5). It remained few changes during the UV irradiation process for the three surfaces. After 7 hours, the water contact angles were 114° for the untreated silicone elastomer, and 155° for both of the template and the SHSE that maintained their superhydrophobic property, as shown in Fig. 7(a2, a4 and a6). As we know, the role of surface roughness has been discussed in two famous main models. One is Wenzel's state. The other is Cassie's state.[32] In Cassie's state, the water droplets adopt a non-wet contact mode which can roll off the dirt easily due to air trapped between water droplets and substrates. As a super-hydrophobic self-cleaning surface, it should have the ability to get rid of dirt during the water droplet rolling process. As shown

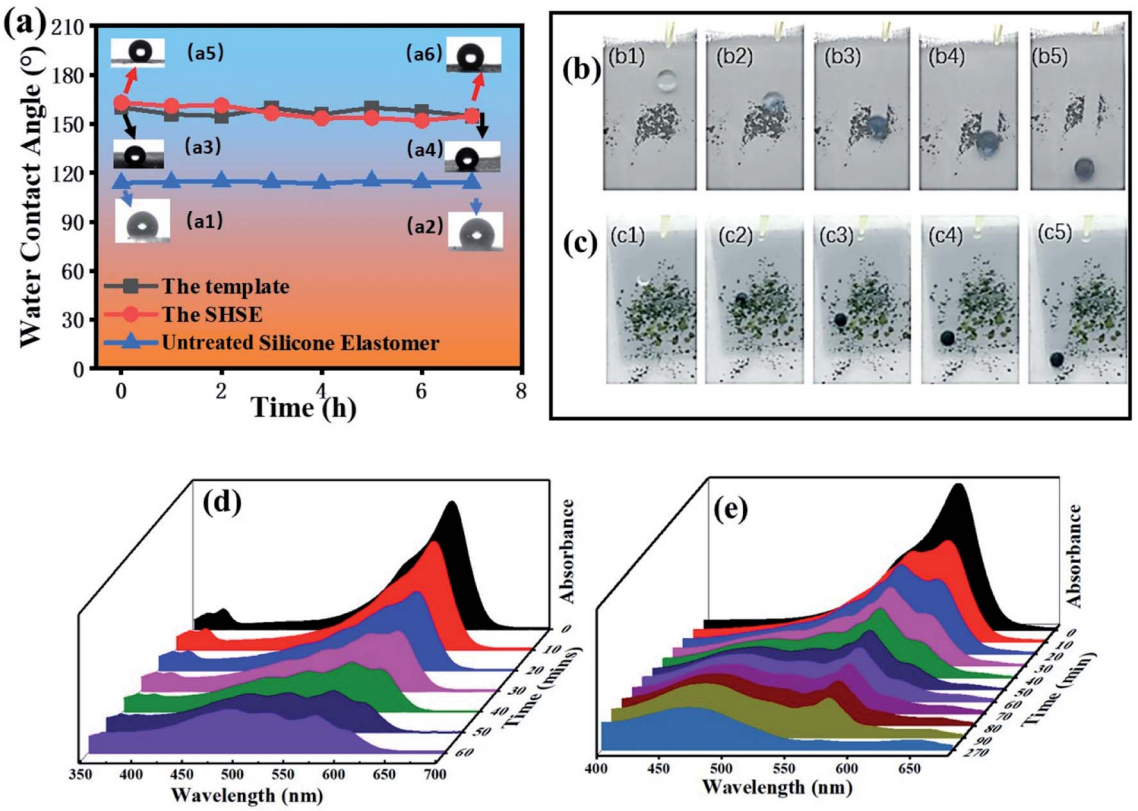

Fig. 7 (a) The WCA changes against UV irradiation time of 7 hours. (a1, a3 and a5) Initial WCA of the untreated silicone elastomer, the template and the SHSE; (a2, a4 and a6) the WCA after 7 hours for the untreated silicone elastomer, the template and the SHSE. Still images from the video of rolling off MB particles process (b1–b5) with a 50 μL water droplet on the homemade template and (c1–c5) with a 20 μL water droplet on the template formed silicone elastomer, both of them were attached to a white board tilted by 10°. UV-vis spectra for samples treated with resazurin dye solution: (d) the homemade template; (e) the SHSEs.

in Fig. 7(b1–b5), the rolling process shows that the template is superhydrophobicity in Cassie's state and has a practical self-cleaning function. The same phenomenon happened in template-assisted formed silicone elastomer. It is also in Cassie's state that the MB powders were rolled off apparently during water rolling, as it showed in Fig. 7(c1–c5). Interestingly, this phenomenon indicated that the homemade template structure was successfully copied from the template to the surface of the silicone elastomer.

Resazurin is blue, and it is readily reduced to a pink reduced form called resorufin.[33] The photocatalytic activity of both the homemade template and templated assisted SHSEs were tested against the breakdown of resazurin dye molecules.[34,35] Generally, the removal of organic pollutants occurs as follows: when the energy of the excitation source is higher than the bandgap of TiO_2, photoexcited electrons and holes are generated. The photoexcited electrons can reduce the oxygen to form superoxide radicals or hydroperoxyl radicals; moreover, the holes oxidize the adsorbed water or hydroxy into hydroxy radicals.[36] As reported by previous reports,[37,38] these reactive oxygen species can convert MB and Rz into CO_2, H_2O, and other minerals. Fig. 7(d) shows that the template appeared to have an efficient photocatalytic activity which made the dye become discolored after 90 min of UV irradiation. Compared to the template, as shown in Fig. 7(e), the rate of the degradation process of SHSE was slower. It took 210 minutes of irradiation to make Rz dye discoloration. The reason is the content of TiO_2 nanoparticles embedded on the SHSE surface is less than the template, which can also be proved from their corresponding EDS elemental analysis in Fig. 4(e and f).

4. Conclusion

We introduce a template-assisted approach to preparing silicone elastomers with excellent superhydrophobic self-cleaning functions and photocatalytic activity. Notably, a bulk elastomer material with multi-functions was obtained during the one-step solidification process. The micro/nano-structure formed by the assistance of the template makes the silicone elastomer surface with an initial WAC at ~163°, which is in Cassie's state that can easily self-clean the surface contamination. Meanwhile, the SHSEs can maintain their excellent hydrophobicity after sandpaper abrasion and show liquid repellency to wine and coffee droplets. Also, the TiO_2 particles transferred from the template make the surface has the photocatalytic activity to degrade Rz dyes and MB dyes in water. This new approach is promising to fabricate multifunctional materials in the one-step molding process.

Conflicts of interest

There are no conflicts to declare.

Acknowledgements

This work is supported by the Natural Science Foundation of Fujian (No. 2021J05249, No. 2019J01829, No. 2019J01830), the Scientific research start-up foundation of Wuyi University (No. YJ202101), and the Scientific and Technological Plan of Guangdong Province, China (2019B090905007); the work is also supported by Qing Yuan HuaYan Institute of Science and Technology Collaborative Innovation, Co., Ltd.

References

1 Y. Almubarak and Y. Tadesse, *Int. J. Intell. Robot. Appl.*, 2017, **1**(3), 352–368.
2 A. J. Mazaltarim, J. M. Taylor, A. Konda, M. A. Stoller and S. A. Morin, *ACS Appl. Mater. Interfaces*, 2019, **11**(36), 33452–33457.
3 M. Schaffner, J. A. Faber, L. Pianegonda, P. A. Rühs, F. Coulter and A. R. Studart, *Nat. Commun.*, 2018, **9**(1), 878–879.
4 C. R. Crick, J. C. Bear, A. Kafizas and I. P. Parkin, *Adv. Mater.*, 2012, **24**(26), 3505–3508.
5 L. Zhang, R. Dillert, D. Bahnemann and M. Vormoor, *Energy Environ. Sci.*, 2012, **5**(6), 7491–7507.
6 T. Kamegawa, Y. Shimizu and H. Yamashita, *Adv. Mater.*, 2012, **24**(27), 3697–3700.
7 I. P. Parkin and R. G. Palgrave, *J. Mater. Chem.*, 2005, **15**(17), 1689–1695.
8 A. Fujishima, X. Zhang and D. A. Tryk, *Surf. Sci. Rep.*, 2008, **63**(12), 515–582.
9 K. Nakata and A. Fujishima, *J. Photochem. Photobiol., C*, 2012, **13**(3), 169–189.
10 J. Rathouský, V. Kalousek, M. Kolář, J. Jirkovský and P. Barták, *Catal. Today*, 2011, **161**(1), 202–208.
11 S. Peng, W. Meng, J. Guo, B. Wang, Z. Wang, N. Xu, X. Li, J. Wang and J. Xu, *Langmuir*, 2019, **35**(7), 2760–2771.
12 Q. F. Xu, Y. Liu, F. J. Lin, B. Mondal and A. M. Lyons, *ACS Appl. Mater. Interfaces*, 2013, **5**(18), 8915–8924.
13 S. Wang, K. Liu, X. Yao and L. Jiang, *Chem. Rev.*, 2015, **115**(16), 8230–8293.
14 Z. Dai, G. Chen, S. Ding, J. Lin, S. Li, Y. Xu and B. Zhou, *Adv. Funct. Mater.*, 2021, **31**(7), 2008574.
15 Y. Cho and C. H. Park, *RSC Adv.*, 2020, **1**(52), 31251–33126.
16 S. Czyzyk, A. Dotan, H. Dodiuk and S. Kenig, *Prog. Org. Coat.*, 2020, **140**, 105501.
17 X. Su, H. Li, X. Lai, L. Zhang, J. Wang, X. Liao and X. Zeng, *ACS Appl. Mater. Interfaces*, 2017, **9**(33), 28089–28099.
18 M. Xi, J. Yong, F. Chen, Q. Yang and X. Hou, *RSC Adv.*, 2019, **9**(12), 665–6657.
19 X. Chen, Y. He, Y. Fan, Q. Yang and H. Li, *Appl. Phys. A: Mater. Sci. Process.*, 2016, **122**(12), 1–10.
20 J.-H. Oh, M.-W. Moon and C. H. Park, *RSC Adv.*, 2020, **1**(18), 1939–1948.
21 L. Xu, L. Yang, S. Yang, Z. Xu, G. Lin, J. Shi, R. Zhang, J. Yu, D. Ge and Y. Guo, *ACS Appl. Mater. Interfaces*, 2021, **13**(5), 6758–6766.
22 C. Li, M. Boban, J. M. Beebe, D. E. Bhagwagar, J. Liu and A. J. Tuteja, *Langmuir*, 2021, **37**(10), 3104–3112.
23 S. Zhai and H. Zhao, *Appl. Phys. Lett.*, 2019, **114**(23), 233702.
24 D. Lv, S. Li, J. Wan, J. Dong and J. Liu, *Polym. Chem.*, 2019, **10**(3), 331–335.

25 Q. Wen and Z. Guo, *Chem. Lett.*, 2016, **45**(10), 1134–1149.
26 L. Gui, J. Lin, J. Liu, J. Zuo, Q. Wang, W. Jiang, T. Feng, S. Li, S. Wang and Z. Liu, *Chem. Eng. J.*, 2022, **431**, 134103.
27 A. Milionis, E. Loth, I. S. Bayer and I. Science, *Adv. Colloid Interface Sci.*, 2016, 57–79.
28 J.-H. Oh, T.-J. Ko, M.-W. Moon and C. H. Park, *RSC Adv.*, 2017, **7**(41), 25597–25604.
29 D. Wang, Q. Sun, M. J. Hokkanen, C. Zhang, F.-Y. Lin, Q. Liu, S.-P. Zhu, T. Zhou, Q. Chang, B. He, Q. Zhou, L. Chen, Z. Wang, R. H. A. Ras and X. Deng, *Nature*, 2020, **582**(7810), 55–59, 59A–59G.
30 Y. Lu, S. Sathasivam, J. Song, C. R. Crick, C. J. Carmalt and I. P. Parkin, *Science*, 2015, **347**(6226), 1132–1135.
31 Y. Lu, S. Sathasivam, J. Song, C. R. Crick, C. J. Carmalt and I. P. Parkin, *Science*, 2015, **347**(6226), 1132–1135.
32 J. Long, L. Pan, P. Fan, D. Gong, D. Jiang, H. Zhang, L. Li and M. Zhong, *Langmuir*, 2016, **32**(4), 1065–1072.
33 A. Mills, J. Wang, S. K. Lee and M. Simonsen, *Chem. Commun.*, 2005, **21**(21), 2721–2723.
34 S. Kundu, A. Kafizas, G. Hyett, A. Mills, J. A. Darr and I. P. Parkin, *J. Mater. Chem.*, 2011, **21**(19), 6854–6863.
35 K. Andreas and I. P. Parkin, *J. Am. Chem. Soc.*, 2011, **133**(50), 20458–20467.
36 S. Banerjee, D. D. Dionysiou and S. C. Pillai, *Appl. Catal., B*, 2015, **176–177**, 396–428.
37 A. Houas, H. Lachheb, M. Ksibi, E. Elaloui, C. Guillard and J.-M. Herrmann, *Appl. Catal., B*, 2001, **31**(2), 145–157.
38 A. Mills and J. Wang, *J. Photochem.*, 1999, **127**(1–3), 123–134.